Morphological Changes of a Molten Polymer/Polymer Interface Driven by Grafting

Jinbao Jiao[†]

Department of Chemistry, Cornell University, Ithaca, New York 14850

Edward J. Kramer*

Department of Materials, University of California, Santa Barbara, Santa Barbara, California 93106

Sicco de Vos[‡] **and Martin Möller**

Department of Organic Chemistry, University of Ulm, Abteilung OC III, Ulm, Germany

Cor Koning

DSM Research, P.O. Box 18, 6160 Geleen, The Netherlands

Received August 10, 1998; Revised Manuscript Received July 2, 1999

ABSTRACT: Whether interfacial tension between two molten polymers can be reduced significantly by the formation of copolymer at the interface by chemical reaction of functionalized chains is the question addressed by this paper. To answer it, model experiments are carried out by grafting of benzylamine end-functionalized deuterated polystyrene (dPS−NH_2) onto poly(styrene-*r*-maleic anhydride) (PSMA) random copolymer at an initially planar melt interface between polystyrene (PS) and PSMA. Various volume fractions of dPS−NH_2 with polymerization indices $N = 33$, 55, and 270 were mixed with PS and then reacted with PSMA above the T_g of PS and PSMA. The interfacial excess, z^*, of the dPS portion of the graft copolymer formed at the boundary was measured using forward recoil spectrometry. The values of normalized grafting density z^*/R_g, where R_g is the radius of gyration of dPS−NH_2, are observed to be as large as 40, 9, and 4 for the $N = 33$, 55, and 270 dPS−NH_2 chains, respectively. These large values signal the formation of a layer of microemulsion which occurs when the interfacial tension of the flat interface is driven negative by the increasing graft copolymer excess at the interface. The interfacial instability is followed by monitoring the positions of Au particles deposited on the original (flat) interface using cross-sectional transmission electron microscopy (TEM). Evidence of the interfacial corrugation induced by the instability is also available from scanning force microscopy (SFM) of the exposed PSMA interface after selective removal of PS using a solvent wash. The length scale of the corrugation is around 200 nm, which is the same magnitude as the size of the emulsion droplets shown by TEM near the interface. The onset of the interface instability occurs at critical values of z^*/R_g of about 1.8 for $N = 55$ and z^*/R_g of about 2.5 for $N = 270$ dPS−NH_2 chains. These values are predicted qualitatively by self-consistent mean field theory.

Introduction

Reactive polymer blending is an increasingly important commercial technique.[1,2] Copolymer generated by the chemical reaction of end-functionalized chains at polymer/polymer melt interfaces can improve the microstructure and properties of polymer blends,[3−5] promote small droplet size by preventing particle coalescence,[6,7] and increase the interfacial fracture toughness.[8,9]

The copolymers generated at the interface form polymeric surfactants with chain tails extending into the two immiscible polymer phases thus decreasing the interfacial tension.[10−13] If enough copolymers are formed at the interface, the interfacial tension of the planar interface can be driven to zero or even slightly negative.[14,15] When the interfacial tension becomes zero, there is no longer a free energy penalty associated with the expansion of the interfacial area. More to the point, the negative tension becomes the driving force for increasing the area of the boundary. Therefore, interfacial fluctuations out of the plane that will cause the unstable interface to expand its area are favored. These fluctuations lead to a corrugated interface. The increased local curvature of the interface can return the interfacial tension to a slightly positive value. On the other hand, when the area increases, the interfacial coverage decreases, which in turn leads to a further grafting of chains at the interface and a subsequent further increase in the interfacial area. These large deformations of the interface may cause droplets to break off from it, thus forming a layer of emulsified droplets near the interface.

It has long been known that spontaneous microemulsion formation can occur at oil/water interfaces, and this microemulsion formation has been studied extensively.[16−20] These microemulsions have been applied in industry to enhance oil recovery.[21] However, the investigation of the microemulsion formation at the polymer melt phase boundaries is still at its incipient stage. Shull et al.[10] first observed a dramatic decrease in interfacial tension at an interface of PS and poly(parahydroxystyrene) (PPHS). This was caused by an addition of a block copolymer of deuterated polystyrene

* To whom correspondence should be addressed.
[†] Current address: Motorola Inc., 4000 Commercial Ave., Northbrook, IL 60062.
[‡] Current address: Akzo Nobel Central Research, Afd RPH, Velperweg 76, P.O. Box 9300, 6800 SB Arnhem, The Netherlands.

10.1021/ma981262c CCC: $18.00
Published on Web 08/21/1999

and poly(2-vinylpyridine) (dPS-*b*-PVP). The strong interaction of PPHS with the PVP block leads to a large segregation of dPS-*b*-PVP from the PS matrix to the interface and a vanishing of the interfacial tension. Recently Xu et al.[22] have directly visualized (by transmission electron microscopy) the morphological consequences of driving the interfacial tension to zero using a similar system to the one investigated by Shull et al. The strong segregation of the dPS-*b*-PVP copolymer, measured as the normalized grafting density z^*/R_g, where z^* is the interfacial excess of the long dPS block and R_g is its radius of gyration, drives the interfacial tension negative and triggers an instability that leads to boundary corrugation and microemulsion formation at $z^*/R_g \approx 3$.

A similar type of instability should result in principle from the formation of graft copolymers by chemical reaction at the boundary. A large z^*/R_g of graft copolymers should be able to be formed at a melt interface by a chemical reaction of end-functionalized polymer chains across the boundary. Theoretical studies relating to the kinetics of such reactions in the melt have been conducted recently.[23−25] As z^*/R_g increases, a free energy barrier (μ^*/k_BT) to the grafting reaction develops due to the entropy loss involved in the localization of the end of the chain at the interface and the stretching of the "brush" of grafted chains. The buildup of such a barrier as z^*/R_g increases will dramatically slow the kinetics of the grafting reaction and ultimately limit the z^*/R_g achievable in practical times. Indeed whether such a grafting reaction can lead to z^*/R_g large enough (1.0−2.5)[26] to produce any significant decrease in interfacial tension is still in doubt. Recent theoretical work[25] based on a scaling analysis valid for large N concludes that before the reaction can position sufficient copolymers at the interface to substantially diminish the interfacial tension, the reaction rates are suppressed to near zero by the increasing μ^*/k_BT barrier.

However, for short functionalized chains, our recent brief communication [27] showed that the theoretical prediction may not hold. We present in this paper much more extensive experimental results and compare these to theoretical predictions for grafting of chains of moderate length comparable to those used in industrial practice. These results show that the grafting density z^*/R_g of such chains can approach very large values. This large z^*/R_g can significantly decrease the interfacial tension. The transition of the interface from flat to corrugated occurs at a critical $z^*/R_g = z_c^*/R_g$. We investigate here this transition by transmission electron microscopy (TEM) and scanning force microscopy (SFM) and find that a simple theoretical model based on a self-consistent mean field (SCF) model can provide a reasonable interpretation of our results.

Experimental Section

Polymers. Benzylamine end functionalized deuterated polystyrenes were prepared by the following process. The anionic polymerization was carried out at room temperature on a high vacuum line fitted with two flasks and a septum.[28] In one of these flasks, 5 g of deuterated styrene monomer and 125 mL of freshly distilled toluene were dried with dibutylmagnesium solution. The solution was degassed twice by freezing−evacuation−thawing cycles and subsequently distilled under vacuum into the other flask. The polymerization was initiated with the addition of a calculated amount of *sec*-butyllithium solution under argon. Polymerizations were completed after 2.5 h under vigorous stirring and without external heating or cooling. *N*-(Trimethylsilyl)benzaldimine (NTSB) was prepared as described in the literature.[29] Prior to the addition of the NTSB, a small sample was taken from the reaction mixture and precipitated in methanol. These dPS−H samples were used to determine the molecular weights and the polydispersities by GPC. The reaction mixture was cooled to −78 °C and the living polystyryl anions were endcapped with a 1.5 molar excess of NTSB. The reaction mixture was left to warm slowly to room temperature overnight. The chain ends were terminated with excess methanol and the benzylamine end group was deprotected by hydrolysis with dilute HCl. After neutralization with base, the polymers were precipitated in methanol, isolated by filtration and dried at 60 °C under vacuum for at least 24 h. The yield of amination, f, was determined quantitatively by ^{1}H NMR and by titration with trifluoromethanesulfonic acid. The results are listed in Table 1.

Table 1. Characteristics of the Grafting DPS−NH_2 Chains

			f	
N	M_n	M_w/M_n	^{1}H NMR	titration
33	3300	1.10	0.99	0.88
55	5500	1.11	0.60	0.59
270	27300	1.13	0.75	0.89

Sample Preparation. Samples for the grafting experiments were prepared as follows: Films about 0.5−1 μm thick of PSMA were spun cast from methyl isobutyl ketone solution onto silicon wafers and dried in a vacuum at 80 °C. The PSMA was manufactured via a free radical polymerization procedure by DSM. According to the manufacturer its maleic anhydride content is 28 wt %, its weight-average molecular weight is M_w = 110K and its polydispersity index is $M_w/M_n = 2.1$. To cover the layer of dPS−NH_2 on PSMA surface, two methods were used. When the volume fraction of dPS−NH_2 in PS was low ($\varphi_0 < 0.5$), we used a float transfer method in which a film about 0.4 μm thick of a mixture of the dPS−NH_2 chains and protonated PS chains (M_n = 107 000 and $M_w/M_n < 1.1$) were spun cast from toluene solutions on a glass slide and floated on the surface of water. The films were then picked up using the PSMA-coated wafer. When the volume fraction of dPS−NH_2 in PS was high ($\varphi_0 > 0.5$), this method was difficult due to the low molecular weight of dPS−NH_2. In this case, we spun cast a layer of dPS−NH_2/PS from toluene directly on the PSMA-coated wafers. The toluene did not dissolve or significantly swell the PSMA film. The initial volume fraction φ_0 of dPS−NH_2 in the PS was varied from 0 to ∼ 0.9 which varied the initial chemical potential of the dPS−NH_2 in the top layer of the bilayer film. After drying, these bilayer films were annealed at temperatures above the glass transition temperature T_g of both PS (100 °C) and PSMA (163 °C) for various times in a vacuum to allow grafting to occur. Grafting is expected to occur by reaction of the amine end with an anhydride group on the PSMA to first form an amic acid and followed by ring closure to form an imide[30] as shown in Scheme 1. Because of the high T_g of our PSMA and the relatively low grafting temperature, however, we believe that the grafting reaction in our case stops at the formation of the amic acid (AB). At low initial dPS−NH_2 volume fractions, the grafting reaction is observed to be completely reversible,[31] which should not be the case if imidization had occurred.

Methods. Grafting was detected by analyzing the deuterium depth profile by forward recoil spectrometry (FRES).[32] A typical FRES depth profile is shown in Figure 1. In the first method the interface excess z^* of dPS−NH_2 was determined as

$$z^* = \int (\varphi(z) - \varphi_\infty)\, dz \qquad (1)$$

where z is the depth from the interface and φ_∞ is the volume fraction of dPS−NH_2 in the bulk of the PS film away from the interface.[33] In the second method, the bilayer film was washed in cyclohexane to remove all the PS and unreacted dPS−NH_2 chains. Now z^* was determined from the depth profile as the

Scheme 1

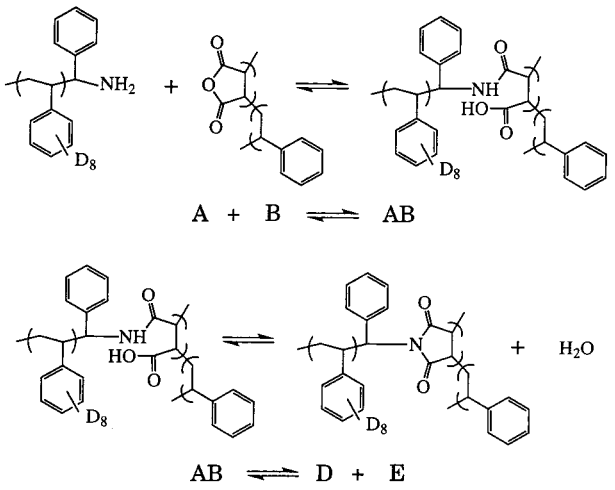

integral of dPS at the surface of the washed PSMA film.[9] The z^*s measured by both methods were in good agreement for the $N = 270$ dPS−NH_2 chains for all initial volume fractions φ_0 and for the $N = 55$ chains for initial volume fractions φ_0 less than 0.1. For $N = 55$ chains at higher volume fractions and long reaction times, z^* from method 1 was usually larger than z^* from method 2. The reason for this discrepancy will be discussed in the last section of this paper. For $N = 33$ chains, method 2 was used exclusively at large φ_0 since z^* was too small to detect reliably at the interface against the background of ungrafted dPS−NH_2 chains.

Transmission Electron Microscopy And Scanning Force Microscopy. Samples for transmission electron microscopy (TEM) were prepared by spin casting 0.4 μm thick films of PSMA onto an epoxy substrate, and floating a layer of dPS−NH_2 (mixed to produce various values of φ_0 in PS) on top the PSMA surface. The bilayers were then annealed at least 72 h at the temperature of interest. In some samples, a thin, discontinuous layer (~5 Å average thickness) of Au particles were formed by thermal evaporation of Au in a vacuum on the surface of PSMA before the float transfer of the dPS−NH_2 layer. Cross-sections 60−90 nm thick were cut normal to the interface using a Reichert Ultracut S microtome. Microtomy was conducted at room temperature using fresh glass knives. Sections were picked up on 400-mesh uncoated gold grids; some sections were stained in a vapor of RuO_4 (5% aqueous solution) for 5 min. This treatment selectively stains the phenyl ring of PS (but also the 70 mol % S in the PSMA),[34] which causes the PS to appear darker than PSMA in the micrographs presented here. TEM was performed using a JEOL 1200SX electron microscope operated at 120 kV.

The topography of the interface was examined by scanning force microscopy (SFM) after selectively washing away the ungrafted chains of dPS−NH_2 and the PS matrix from the top surface of the PSMA layer. Bilayers of the grafting polymers were first prepared on a 1 × 1 cm^2 silicon wafer and annealed as described above. Samples were then washed in 50 mL of cyclohexane in an ultrasonic bath at room temperature for 20 min and dried in air. A Nanoscope-II SFM from Digital Instruments with a pyramidal Si_3N_4 tip (nominal spring constant of 0.12 N m^{-1}) was used for all SFM measurements.

Results and Discussion

We first examined the time dependence of grafting at an initial volume fraction $\varphi_0 \sim 0.06$ for the $N = 270$ and $N = 55$ chains of dPS−NH_2 on an initial planar interface with PSMA. For both $N = 270$ and $N = 55$ the bulk volume fractions measured experimentally were corrected for the fraction f (from f ^{1}H NMR of Table 1) of dPS chains actually terminated by amine groups. The grafting kinetics at 170 °C for dPS−NH_2 chains with $N = 55$ and $N = 270$ are shown in Figure 2a and

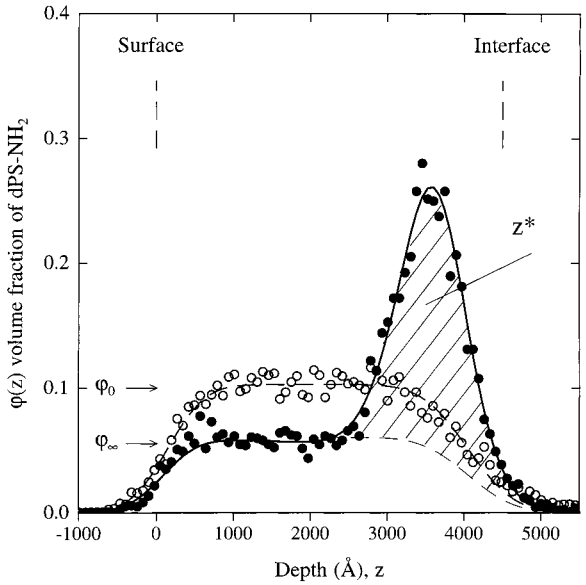

Figure 1. Volume fraction vs depth profile of $N = 270$ dPS−NH_2 in a blend of dPS−NH_2 and PS at an interface with PSMA. Open circles (○) show the depth profile of dPS−NH_2 in PS from the surface to the interface prior to the annealing with an initial volume fraction of 0.1; Filled circles (●) show the concentration profile of dPS−NH_2 after annealing at 190 °C for 72 h. After the annealing, the volume fraction in the bulk PS blend is φ_∞. The interfacial integral excess z^* is represented by the shaded area.

Figure 2b as z^*/R_g vs annealing time. Both sets of data can be fitted by expressions of the following type

$$z^*/R_g = A(1 - \exp(-t/\tau)) \qquad (2)$$

where A and τ are constants for that particular grafting temperature and N value. For the $N = 270$ dPS−NH_2 the values of τ and A are 25 h and 1.75. But for $N = 55$ a characteristic time $\tau \sim 250$ h and an A of 12 are required to produce the line shown in Figure 2. The roughly 10-fold increase in characteristic time with a 5-fold decrease in N alerts us to the possibility that something unusual is happening for at least one of these samples. All of the theoretical treatments of end-functionalized chain grafting at a planar interface[23−25] would predict a decrease in characteristic reaction time with a decrease in N of the grafting chain.

The sense of something unusual is reinforced by the results shown in Figure 3 where the z^*/R_g after a long grafting time (72 h) at 190 °C is plotted vs the bulk volume fraction of the dPS−NH_2 in PS measured experimentally. These results were obtained after the bilayer film was washed in cyclohexane to remove all the PS and unreacted dPS−NH_2 chains and the grafting time was sufficient such that no further changes in the z^*/R_g were observed at long grafting times. Again grafting of the $N = 270$ dPS−NH_2 chains proceeds apparently normally with z^*/R_g increasing monotonically with increasing φ_∞. But for both the $N = 55$ and $N = 33$ dPS−NH_2, the z^*/R_g first increases with φ_∞, goes through a maximum and then decreases to a value of about 4. The maximum value of z^*/R_g is as large as 42 for the $N = 33$ chains and 6 for the $N = 55$ chains.

Values of z^*/R_g greater than 3 resulting from the segregation of block copolymers to polymer/polymer interfaces have been attributed to interface instability and microemulsion formation.[10,22] These previous experiments suggest that the large values of z^*/R_g ob-

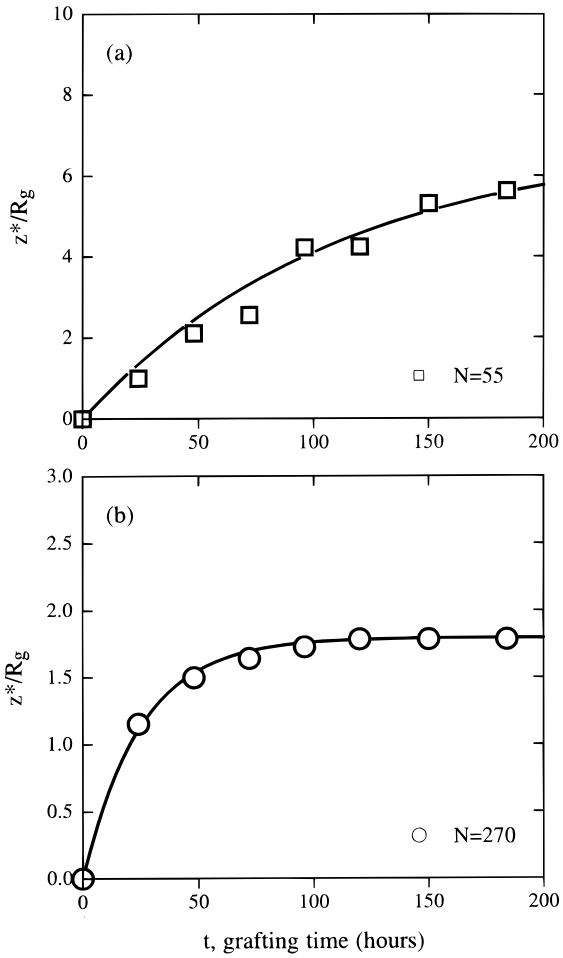

Figure 2. Grafted integral excess z^* normalized by R_g vs grafting time at 170 °C for dPS−NH_2 with different degrees of polymerization of (a) $N = 55$ and (b) $N = 270$. The volume fraction of dPS−NH_2 is $\varphi_0 = 0.06$ for $N = 55$ and $\varphi_0 = 0.075$ for $N = 270$.

served in our grafting experiments are caused by a similar decrease in interfacial tension leading to interface instability as the graft copolymer at the interface builds up. On the basis of the Gibbs adsorption equation, the increase in the interfacial excess of copolymer chains at the interface is accompanied by a decrease in interfacial tension given approximately by[10]

$$\gamma = \gamma_0 - \frac{\rho_0 R_g k_B T}{N} \int_{-\infty}^{\mu} \frac{z^*(\mu)}{R_g} \, d\mu \tag{3}$$

where γ_0 is the initial interfacial tension without the graft copolymers, ρ_0 is the segment density of dPS−NH_2, N is the chain length of the dPS portion of copolymer at the interface, k_B is Boltzmann's constant, and μ is the chemical potential of the grafted copolymer.

The decrease in interfacial tension can be written in the following form:

$$-\frac{\Delta\gamma}{k_B T} = \frac{\rho_0 a}{\sqrt{6N}} \alpha(z^*/R_g) \tag{4}$$

Here, a is the statistical segment length of the polymer and α is a function of z^*/R_g tabulated by Shull[26] from his self-consistent mean field calculations valid for the case when the unreactive matrix chains are much longer than the end-functional chains. At large z^*/R_g, the

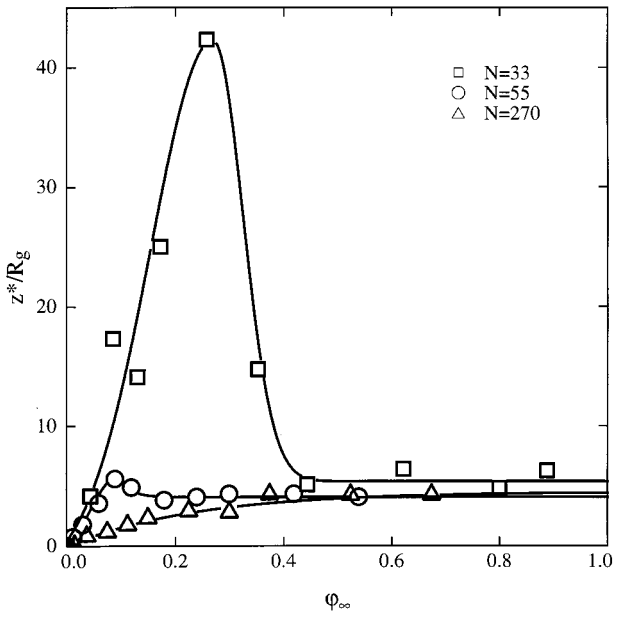

Figure 3. Grafted integral excess z^* (after washing with cyclohexane) normalized by R_g vs volume fraction of dPS−NH_2 left in PS. Reaction was carried out at 190 °C in a vacuum for 72 h. $N = 270$ dPS−NH_2 (triangles); $N = 55$ dPS−NH_2 (squares); $N = 33$ dPS−NH_2 (circles).

function α is approximately $0.5(z^*/R_g)^3$, a result first obtained by Leibler.[11] Equation 4 does not consider the loss in entropy of the PSMA chains to which the dPS−NH_2 chains are grafted and so is a lower limit for $-\Delta\gamma/(k_B T)$.

The tension γ_0 for an interface between high molecular weight polymers without graft copolymers can be found from the result of Helfand and Tagami[35]

$$\frac{\gamma_0}{k_B T} = \rho_0 a \sqrt{\frac{\chi}{6}} \tag{5}$$

where χ is the Flory−Huggins interaction parameter. Corrections for finite molecular weight will only decrease γ_0. Dividing eq 4 by eq 5, we arrive at an expression for the ratio of the decrease in interfacial tension to the initial interfacial tension.[27]

$$-\frac{\Delta\gamma}{\gamma_0} = \frac{1}{\sqrt{\chi N}} \alpha(z^*/R_g) \tag{6}$$

The effective Flory−Huggins parameter between PS and PSMA is expected to be comparable to $\chi \sim 0.1$ for the strongly immiscible polymers, PS and poly(2-vinylpyridine). As an estimate,[36] we use $\chi = 0.125$ in eq 6 to obtain a prediction of the $-\Delta\gamma/\gamma_0$ vs z^*/R_g for three dPS−NH_2 chains as shown in Figure 4. Note that $-\Delta\gamma/\gamma_0$ should exceed 1, signifying a negative interfacial tension for the flat interface, above a critical value of $z_c^*/R_g = 1.3$ for the $N = 33$ chains, above $z_c^*/R_g = 1.5$ for the $N = 55$ chains, and above $z_c^*/R_g = 2.4$ for the $N = 270$ chains. At these critical values of z_c^*/R_g the grafting potential barrier $\mu^*/(k_B T)$ is approximately 2.8 for $N = 33$, 3.4 for $N = 55$, and 5.5 for $N = 270$.[23] Values of z^*/R_g up to 3 were observed for $N = 840$ dPS−COOH chains grafting on flat epoxy interfaces,[9] which implies a final $\mu^*/(k_B T)$ barrier of about 9. At the values of N used in our present experiments, the $\mu^*/k_B T$ barrier is not so high as to prevent further reaction at the critical z^*/R_g values.

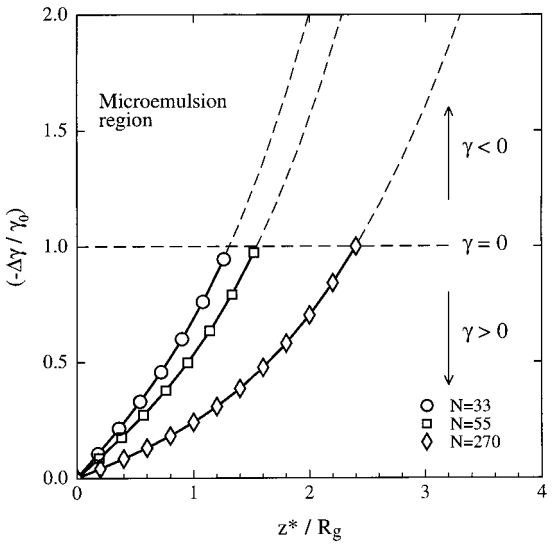

Figure 4. Ratio of the predicted decrease in interfacial tension to the interfacial tension of the unreacted interface as a function of z^*/R_g. $N = 270$ dPS−NH_2 (diamonds); $N = 55$ dPS−NH_2 (circles); $N = 33$ dPS−NH_2 (squares). The interfacial tension is predicted to vanish at critical values of z_c^*/R_g of 2.5, 1.5, and 1.3, respectively.

Therefore, the large z^*/R_g values in Figures 2 and 3 correspond to interfaces that, if they were flat, should have negative interfacial tension. Such an interface would be unstable, and low amplitude waves on the interface would grow.[37] A highly corrugated interface like that observed for large z^*/R_g of block copolymer segregation[22] should result.

Scanning force microscopy provides direct evidence for the spontaneous corrugation of the interface. In this case the PS and unreacted dPS−NH_2 are selectively removed by washing with cyclohexane. The interfacial topography was measured for $N = 55$ samples with different initial dPS−NH_2 volume fractions, φ_0, of 0.006 (not shown, the interface is flatter than Figure 5a), 0.018 (Figure 5a), 0.030 (Figure 5b), 0.042 (Figure 5c), 0.060 (Figure 5d), 0.09 (Figure 5e), and 0.24 (Figure 5f) after annealing at 190 °C for 72 h. As shown in parts a−f of Figure 5, while the interface at low z^*/R_g ($z_w^*/R_g < 1$, e.g. Figure 5a) is very smooth, the interface at z^*/R_g much larger than the critical value ($z_w^*/R_g > 1.8$. e.g. Figure 5c) is very rough with the scale of the lateral roughness being ∼50 nm. The transition of the interface from flat to corrugated was measured by determining the root-mean-square (rms) surface roughness. The variation of the rms roughness with z^*/R_g is plotted in Figure 6 for the $N = 55$ and the $N = 270$ dPS−NH_2 chains. There is a sharp increase in the roughness corresponding to $z_c^*/R_g \sim 2.5$ for $N = 270$ and $z_c^*/R_g \sim 1.8$ for $N = 55$. These results agree qualitatively with the theoretical prediction (Figure 4) that predicts the transition at z^*/R_g values of 2.4 and 1.5, respectively, for $N = 270$ and $N = 55$ chains. The characteristic height of the largest features in parts c and d of Figure 5d is ∼50 nm, and these peaks are spaced about 200 nm apart. It is likely however that SFM does not measure accurately the depth of the deeply corrugated valleys such as those in Figure 5f.

While the detailed kinetics of the development of these corrugations is a matter for future investigation, it seems clear that the overall of roughening is controlled by the viscosity of the more viscous of the two phases (PSMA in our case).[37] That is probably the reason for the very slow increase in z^*/R_g for the $N = 55$ sample at 170 °C shown in Figure 2. Because 170 °C is only 7 °C above the T_g of PSMA, the melt should be very viscous at this grafting temperature.

Also, the actual area of the corrugated interface is much larger than the initial area of the interface in the bilayer film. The FRES measurement integrates over the entire corrugated interface and thus the local z^*/R_g is probably much closer to the critical value where $-\Delta\gamma/\gamma_0$ exceeds 1. This expectation is in agreement with the proposal of de Gennes and Taupin[38,39] who suggest that when the interfacial tension $\gamma = 0$ in a small molecule fluid microemulsion, the system will adopt a well-defined interfacial area a^* per surfactant. Then, the new area of interface (and thus the z^*/R_g measured by FRES) is given by the product of a^* and the number of surfactant molecules (graft copolymers in this case) formed at the interface.

The increased interfacial area in turn enhances the further grafting of the dPS−NH_2. Thus, the apparent grafting density, measured by our FRES depth profiling technique, which averages laterally over the entire corrugated interface, is much higher than that at a locally flat region of that corrugated interface. The apparently low reaction rate of the $N = 55$ chains at 170 °C is due to the dynamic emulsification process which is controlled by the viscous flow of the PSMA phase. As an example, a decrease in viscosity at higher temperatures, e.g. 180 °C, leads to a rapid decrease of characteristic reaction time for $N = 55$ chains from 120 (Figure 2a) to 20 h (Figure 7a). In comparison, the grafting reaction without the microemulsion formation (e.g., at an initial volume fraction $\varphi_0 = 0.012$) approaches saturation ($z^*/R_g \sim 0.5$) in a fairly short time ($\tau = 2$ h) at 180 °C. The time dependence of the z^*/R_g for $\varphi_0 = 0.012$ is plotted in Figure 7b.

Finally, it remains to be explained why a maximum is observed for z^*/R_g in Figure 3. In the case of $N = 55$ it is possible to measure z^* both before and after washing. When z^*/R_g is much larger than the critical value, for example where the interface roughening kinetics are controlled by the viscosity of the PSMA but the kinetics of local grafting are fast (small N), it seems that small spherical particles of graft copolymer coated PSMA may be formed around the interface by pinching off the ends of protruding fingers of the PSMA. These particles will be released into the cyclohexane washing liquid when the PS is dissolved away, carrying with them the dPS−NH_2 chains that are grafted to their surfaces. The decrease in the z^*/R_g at φ_0 beyond the maximum in Figure 3 is thus likely due to the formation of small dPS−NH_2 grafted droplets in the PS phase. Evidence for particles being washed off is also seen in the SFM micrographs for interfaces formed from PS-(dPS−NH_2) mixture with $\varphi_0 \sim 0.15$ (parts e and f of Figure 5). In such interfaces, there are holes observed on the PSMA surface after the washing procedure. These holes may correspond to the regions from which particles were removed by the washing procedure.

Direct evidence that washing removes some originally grafted chains comes from Figure 8a showing the increase in z^*/R_g for the $N = 55$ chains as a function of time for $\varphi_0 = 0.06$. The z^*/R_g measured before washing at long times is more than twice that measured after washing. For much lower initial volume fractions ($\varphi_0 = 0.009$) of $N = 33$ chains (Figure 8b), where no interface

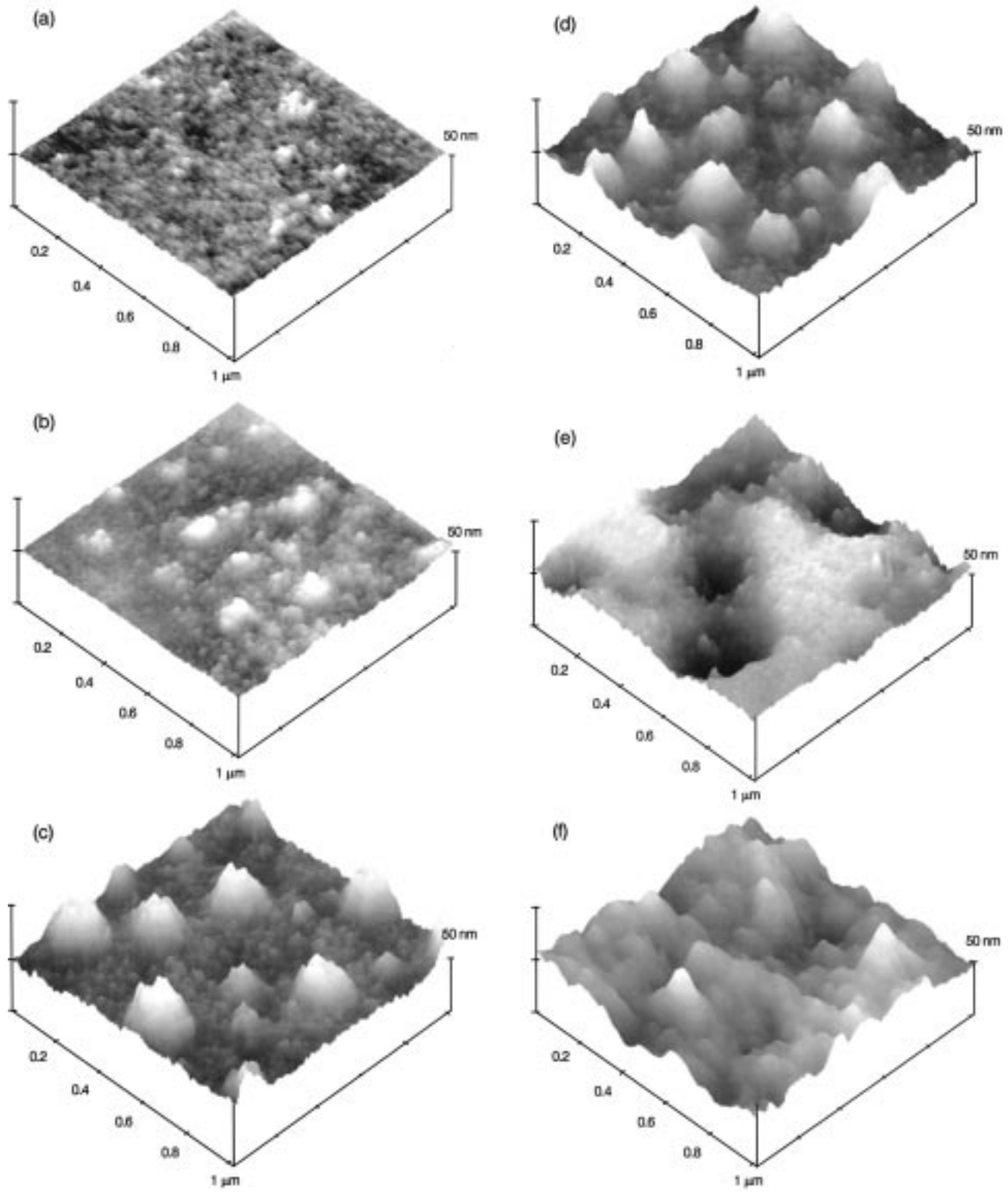

Figure 5. SFM image of the grafted PS/PSMA interface for various values of initial volume fraction (corresponding values of z^*/R_g are plotted in Figure 6) of $N = 55$ dPS−NH_2 after washing with cyclohexane. Key (a) $\varphi_0 = 0.018$, $z_w^*/R_g = 1.3$; (b) $\varphi_0 = 0.030$, $z_w^*/R_g = 1.8$; (c) $\varphi_0 = 0.042$, $z_w^*/R_g = 2.6$; (d) $\varphi_0 = 0.060$, $z_w^*/R_g = 4.0$; (e) $\varphi_0 = 0.09$, $z_w^*/R_g = 5.5$; (f) $\varphi_0 = 0.24$, $z_w^*/R_g = 4.1$.

corrugation or particle formation is expected, the z^*/R_g before washing is the same as the z^*/R_g after washing.

Further evidence of the interface morphology at high z^*/R_g comes from cross-sectional transmission electron microscopy (TEM). Figure 9 shows the cross-sectional TEM micrograph of the interface of a sample grafted at 190 °C with $N = 55$ chains at $\varphi_0 = 0.5$ for 72 h. The contrast is produced by staining the phenyl group of PS and PSMA with RuO_4. The darkest region corresponds to the mixture of PS and dPS−NH_2. The PSMA has less phenyl groups and is stained less by the RuO_4. There is no sharp interface, however, just a region about 300 nm wide with intermediate staining between the PSMA and the PS. Within this layer, some of the regions stained less strongly toward the PS side may be the copolymer coated particles of PSMA in the PS. From this TEM micrograph, however, it would seem that there are also copolymer coated particles of PS in the

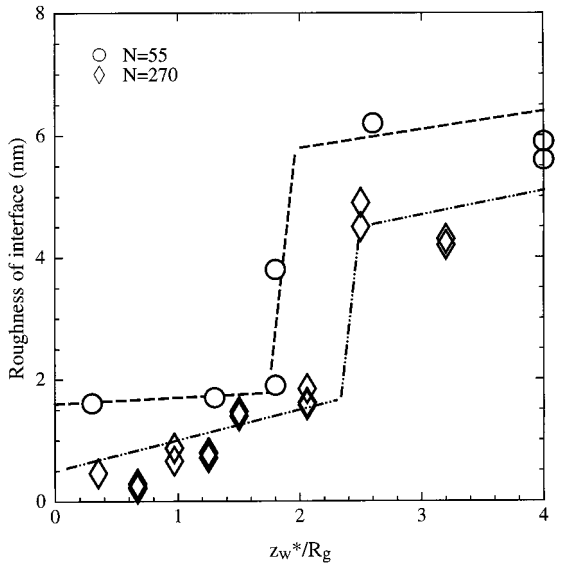

Figure 6. Rms roughness of the interface after removal (by washing with cyclohexane) of the ungrafted chains from the PSMA as a function of the normalized grafting density z^*/R_g. The value of the roughness is from the measured SFM images of the PS/PSMA interface grafted from various initial volume fractions of $N = 55$ and $N = 270$ dPS−NH_2 in PS.

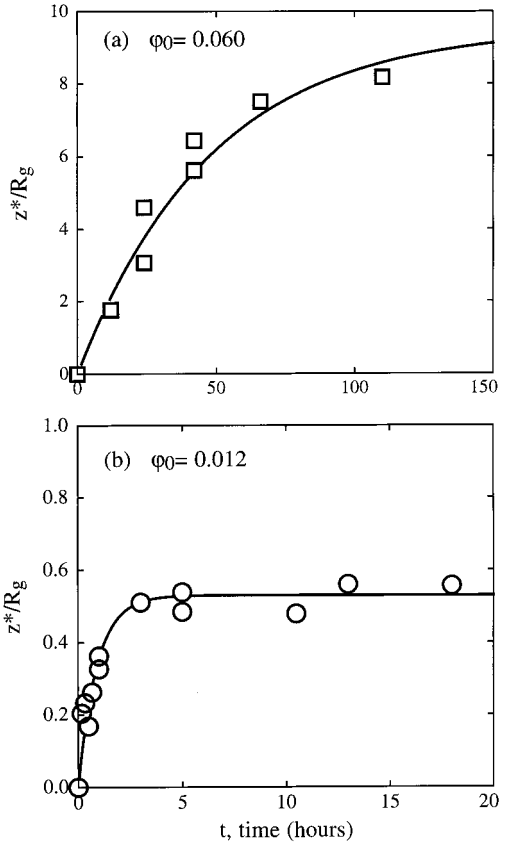

Figure 7. Grafted integral excess z^* (after washing with cyclohexane) normalized by R_g vs grafting time (hours) at 180 °C. Samples of $N = 55$ dPS−NH_2 with different volume fractions of (a) $\varphi_0 = 0.06$ and (b) $\varphi_0 = 0.012$ were used.

PSMA. Since these would not be washed off the interface by cyclohexane, they would still be counted as part of the interfacial excess z^*. Since there is still 70% PS in the PSMA, however, it is clear that RuO_4 staining cannot reveal the droplet structure of the interfacial region very clearly.

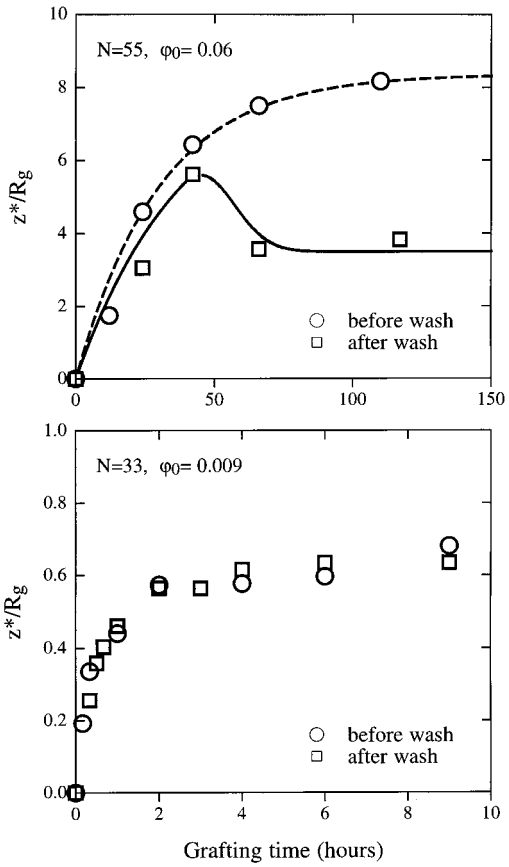

Figure 8. Grafted integral excess z^* (before and after washing with cyclohexane) normalized by R_g vs grafting time (hours). Key: (a) Samples of $N = 55$ dPS−NH_2 with volume fraction of $\varphi_0 = 0.06$ were used. After reaction for over 50 h, the grafting density z_w^*/R_g measured after washing is less than the z^*/R_g measured before washing, which reveals that a droplet formation process is involved at the higher grafting density region ($z^*/R_g > 3$). (b) Samples of $N = 33$ dPS−NH_2 with initial volume fraction of $\varphi_0 = 0.009$ were used. The grafting density z_w^*/R_g measured after washing is the same as the z^*/R_g measured before washing, which reveals that there is no droplet formation process involved at low φ_0 and low z^*/R_g.

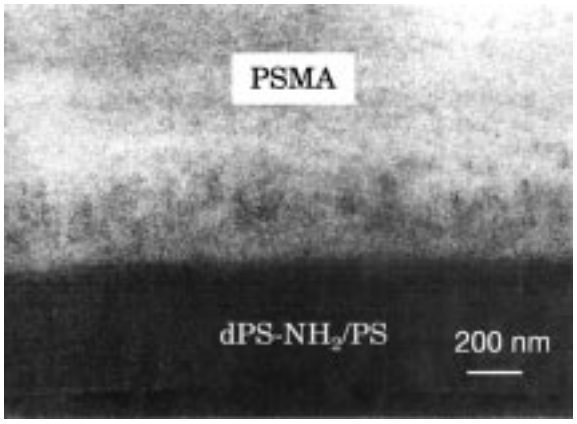

Figure 9. Cross-sectional TEM micrograph of an interface (RuO_4 stained) between PSMA and PS (dPS−NH_2 $N = 33$) after annealing for 72 h at 190 °C. The region at the interface with medium darkness corresponds to the region of the microemulsion. The thickness of this region is about 3000 Å, and the graft copolymer-coated droplets are also revealed to have an average diameter of ∼ 50 nm.

However, very useful information can be obtained by observing Au marker particles formed on the initial PSMA surface by evaporation of a very small amount

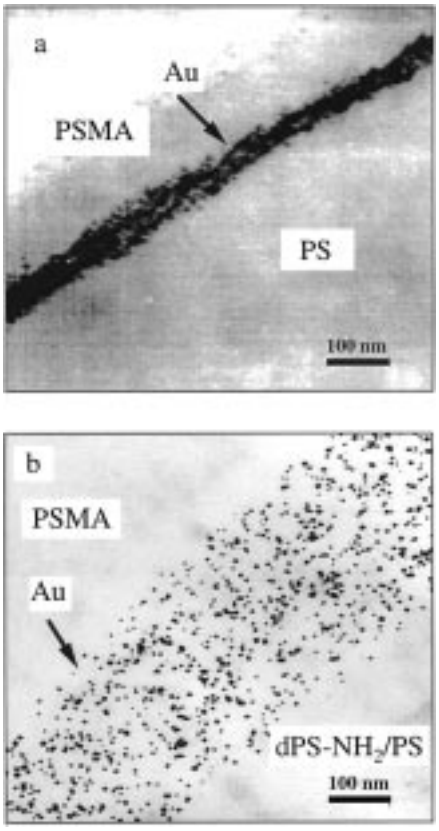

Figure 10. TEM micrograph of a cross-section through a Au particle decorated interface between PSMA and PS after annealing for 72 h at 190 °C. Key: (a) without the addition of dPS−NH_2; (b) with addition of $\varphi_0 = 0.3$ of $N = 55$ dPS−NH_2.

of Au before depositing the film of PS and dPS−NH_2. As a comparison, for one sample no dPS−NH_2 was added to the PS ($\varphi_0 = 0$), whereas another sample consisted of a mixture of $N = 55$ dPS−NH_2 and PS with $\varphi_0 = 0.3$. The two samples were annealed under the same conditions for 72 h. Figure 10a shows the case where no grafting occurs but it is typical of what happens if z^*/R_g is small. In this case the Au particles are very near the original PS/PSMA interface. If z^*/R_g is much larger than the critical value, however, the Au particles are spread out dramatically normal to the original interface as seen in Figure 10b. The implication is that the Au particles are now located along the deeply corrugated interface between the PS and PSMA and at the interfaces of the PS and PSMA microemulsion droplets.

Cross-sectional TEM of samples containing various volume fractions of dPS−NH_2 ($N = 55$) in PS was also carried out to determine the width of the interfacial Au layer. Figure 11 shows the variation of the thickness of the Au particle layer with grafting density z^*/R_g. A jump in Au layer width from <25 nm to >75 nm can be observed at about $z_c^*/R_g = 1.6$. This value is in good agreement with the SFM results. When z_c^*/R_g is less than the critical value 1.6, the Au particle layer is still sharp. Thus, before the transition of the interface from flat to corrugated, the flat interface can accommodate about $z_c^*/R_g = 1.6$ grafted chains. These chains basically form a stretched polymer brush[40] on the PS/PSMA interface and decrease the interfacial tension γ. After the critical value 1.6, $\gamma \sim 0$, the Au layer thickness widens monotonically with the increase of grafting density as the PS/PSMA interface generates spontaneous corrugation to recover a slightly positive interfacial tension. The width of the Au layer continuously increases with the increase of the normalized grafting density above 1.6, whereas the roughness measured using SFM does not show this continuous increase after the interface corrugation (cf. Figure 6). The reason may be due to the following two facts: (1) The tip of the SFM can only measure the roughness of the surface that contacts with the tip.[41] Because the tip has a finite size, the deeply corrugated valleys may not have been measured by SFM, whereas the TEM can reveal these valleys. (2) SFM does not measure the droplets that are washed off from the interface, whereas the interfacial width measured by the thickness of the Au layer from TEM includes all the droplets formed at the interface.

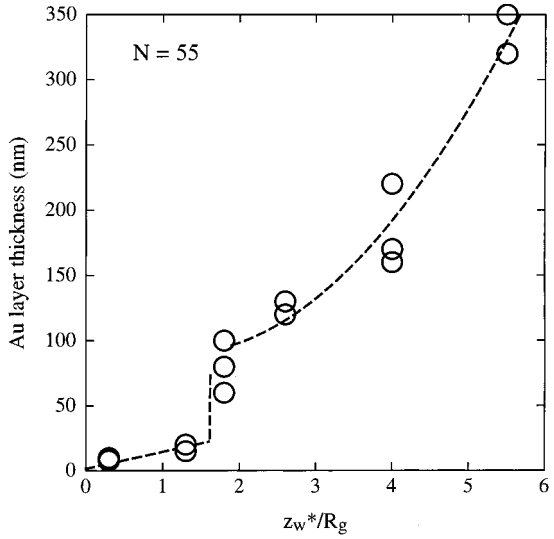

Figure 11. Thickness of the layer of Au particles, originally deposited at the interface of PSMA with PS (dPS−NH_2 $N = 55$), after annealing at 190 °C for 72 h, as a function of normalized grafting density z_w^*/R_g measured after washing. The value of the layer thickness is measured from cross-sectional TEM observations of the sample. A transition is also found at about $z_c^*/R_g \approx 1.6$ and the thickness of the layer of Au particles increases monotonically with the grafting density z_w^*/R_g.

Conclusions

Significant decreases in polymer/polymer interfacial tension are possible by reaction of end-functional chains leading to graft copolymer formation at the interface. This decrease of the interfacial tension can be large enough to drive the tension of the flat interface negative, leading to spontaneous formation of a deeply corrugated interface and eventually graft copolymer coated droplets nearby. The scale of the characteristic curvature (corrugation wavelength) is ~50 nm. The transition of the flat interface to a corrugated one is found to take place at a certain critical grafting density of $z^*/R_g = z_c^*/R_g$. At this critical value the interfacial tension vanishes. Shorter chains have smaller values of z_c^*/R_g. For chains of moderate or small length, this critical z_c^*/R_g can be attained before the increase in the μ^*/k_BT barrier to grafting due to build up of the brush decreases the reaction rate at the interface to near zero. These results show that grafting shorter functional chains leads to an interfacial instability at lower z_c^*/R_g. A simple theoretical model based on the self-consistent mean field theory is used to interpret the formation of the microemulsion as well as the transition from a flat interface to a highly

corrugated interface at the critical grafting density z_c^*/R_g. It predicts that the decrease of the interfacial tension at a constant z^*/R_g is proportional to $(\chi N)^{-1/2}$. The model predicts critical values of z_c^*/R_g at which the interfacial tension vanishes that are in reasonable agreement with the experimental results.

Acknowledgment. We acknowledge the support of the Cornell Materials Science Center (NSF-DMR-MRSEC Grant No. 9632275) under its Polymer Outreach Program through fellowship support from Xerox and Universal Instruments and for the use of its Ion Beam Analysis Central Facility. The skillful help of Peter Revesz and Nick Szabo of this facility are greatly appreciated. The work of S.d.V. was supported by Senter IOP-MT Recycling, The Netherlands. E.J.K. acknowledges support from the UCSB Materials Research Lab (NSF-DMR-MRSEC Grant No. DMR96-32716).

References and Notes

(1) Epstein, B. N. U.S. Patents, 4,174,358 and 4,172,859, 1979.
(2) Jalbert, R. L.; Grant, T. S. U.S. Patent, 4,654,405, 1987.
(3) Stewart, M. E.; George, S. E.; Miller, R. L.; Paul, D. R. *Polym. Eng. Sci.* **1993**, *33*, 675.
(4) Ide, F.; Hasegawa, A. *J. Appl. Polym. Sci.* **1974**, *18*, 963.
(5) Utracki, L. A.; Weise, R. A. *Multiphase Polymers: Blends and Ionomers*; American Chemical Society: Washington, DC, 1989.
(6) Sundararaj, U.; Macosko, C. W. *Macromolecules* **1995**, *28*, 2647. Nakayama, A.; Inoue, T.; Guégan, P.; Macosko, C. W. *Polym. Prepr. (Am. Chem. Soc., Div. Polym. Chem.)* **1993**, *34*, 840. Vaidya, U.; Wolske, K. A.; Sasaki, Y.; Tirrell, M.; Macosko, C. W. *Polym. Prepr. (Am. Chem. Soc., Div. Polym. Chem.)* **1988**, *29*, 561.
(7) Beck Tan, N. C.; Tai, S. K.; Briber; R. M. *Polymer* **1996**, *37*, 3509.
(8) Boucher, E.; Folkers, J. P.; Hervet, H.; Léger, L.; Creton, C. *Macromolecules* **1996**, *29*, 774.
(9) Norton, L. J.; Smigolova, V.; Pralle, M. U.; Hubenko, A.; Dai, K. H.; Kramer, E. J.; Hahn, S.; Berglund, C.; DeKoven, B. *Macromolecules* **1995**, *28*, 1999.
(10) Shull, K. R.; Kellock, A. J.; Deline, V. R.; MacDonald, S. A. *J. Chem. Phys.* **1992**, *97*, 2095.
(11) Leibler, L. *Makromol. Chem., Macromol. Symp.* **1988**, *16*, 1.
(12) Noolandi, J.; Hong, K. M. *Macromolecules* **1982**, *15*, 482.
(13) Noolandi, J.; Hong, K. M. *Macromolecules* **1984**, *17*, 1531.
(14) Landau, L. D.; Lifshitz, E. M. *Statistical Physics*; Pergamon: Oxford, England, 1980; Chapter XV.
(15) Granek, R.; Ball, R. C.; Cates, M. E. *J. Phys. II Fr.* **1993**, *3*, 829.
(16) Hoar, T. P.; Schulman, J. H. *Nature (London)* **1943**, *102*, 152.
(17) Corti, M.; Degiorgio; V. *Physics of Amphiphiles: Micelles, Vesicles and Microemulsion*; North-Holland: Amsterdam, 1985.
(18) Gelbart, W. M.; Roux, D.; BenShaul, A. *Micelles, Membranes, Microemulsions and Monolayers*; Springer-Verlag: New York, 1994.
(19) Overbeek, J. T.; de Bruyn, P. L.; Verhoeckx, F. In *Surfactants*; Tadros, Th. F., Ed.; Academic: London, 1984; Chapter 5; Neustadter, E. L. In Chapter 11.
(20) Benton, W. J.; Raney, K. H.; Miller, C. A. *J. Colloid Interface Sci.* **1986**, *110*, 363. Raney, K. H.; Benton, W. J.; Miller, C. A. *J. Colloid Interface. Sci.* **1987**, *117*, 282. Raney, K. H.; Miller, C. A. *J. Colloid Interface. Sci.* **1987**, *119*, 539.
(21) Shah, D. O.; Schechter, R. *Improved Oil Recovery by Surfactant and Polymer Flooding;* Academic Press: New York, 1977.
(22) Xu, Z.; Jandt, K.; Kramer, E. J.; Edgecombe, B. D.; Fréchet, J. M. J. *J. Polym. Sci.—Polym. Phys.* **1995**, *33*, 2351.
(23) Kramer, E. J. *Isr. J. Chem.* **1995**, *35*, 49.
(24) Fredrickson, G. H. *Phys. Rev. Lett.* **1996**, *76*, 3440. Fredrickson, G. H.; Milner, S. T. *Macromolecules* **1996**, *29*, 7386.
(25) O'Shaughnessy, B.; Sawhney, U. *Phys. Rev. Lett.* **1996**, *76*, 3444; *Macromolecules* **1996**, *29*, 7230.
(26) Shull, K. R. *J. Chem. Phys.* **1991**, *94*, 5723.
(27) Jiao, J.; Kramer, E. J.; de Vos, S.; Möller, M.; Koning, C. *Polym. Commun.* **1999**, *40*, 3585.
(28) Hirao, A.; Hattori, I.; Sasagawa, T.; Yamaguchi, K.; Nakahama, S. *Makromol. Chem., Rapid Commun.* **1982**, *3*, 59.
(29) Hart, D. J.; Kanai, K.; Thomas, D. G.; Yang, T.-K. *J. Org. Chem.* **1983**, *48*, 289.
(30) Scott, C.; Macosko, C. W. *J. Polym. Sci.—Polym. Phys.* **1994**, *32*, 205.
(31) Jiao, J. Ph.D. Thesis, Cornell University, 1997, Chapter 2.
(32) Mills, P. J.; Green, P. F.; Palmstrøm, C. J.; Mayer, J. W.; Kramer, E. J. *Appl. Phys. Lett.* **1984**, *45*, 957.
(33) Shull, K. R.; Kramer, E. J.; Hadziioannou, G.; Tang, W. *Macromolecules* **1990**, *23*, 4780.
(34) Lewis, P. R.; Knight, D. P. In *Practical Methods in Electron Microscopy*; Glauert, A. M., Ed.; Elsevier: Netherlands, Vol. 14 **1992**.
(35) Helfand, E.; Tagami, Y. *Polym. Lett.* **1971**, *9*, 741.
(36) The Flory—Huggins parameter for styrene and maleic anhydride segments χ_{S-MA} has been estimated to be large and positive (~1.7) (Aoki, Y. *Macromolecules* **1988**, *21*, 1277.). For our PSMA, the volume fraction ϕ_{MA} of MA in PSMA (28 wt % MA) is 0.21, and $\chi_{PS-PSMA} = \phi_{MA}^2\chi_{S-MA}$, which gives $\chi_{PS-PSMA} \approx 0.075$. Other workers (Pionteck, J.; Kressler, J. *Proceedings of the European Physical Society Conference on Surfaces and Interfaces in Polymers and Composites*; Lausanne, Switzerland, 1997) find somewhat higher values for χ_{S-MA} which give a $\chi_{PS-PSMA}$ value close to our assumed 0.125.
(37) Granek, R.; Ball, R. C.; Cates, M. E. *J. Phys. II (Fr.)* **1993**, *3*, 829.
(38) de Gennes, P. G.; Taupin, C. *J. Phys. Chem.* **1982**, *86*, 2294.
(39) Taupin, C. *Physics of Amphiphiles: Micelles, Vesicles and Microemulsion*; Corti, M., Degiorgio, V., Eds.; North-Holland: Amsterdam, 1985; pp 757—767.
(40) Milner, S. T. *Science* **1991**, *251*, 4996.
(41) Mori, O.; Imae, T. *Langmuir* **1995**, *11*, 4779.

MA981262C